

Wafer Level Integration of a 24 GHz Differential SiGe-MMIC Oscillator with a Patch Antenna using BCB as a Dielectric Layer

P. Abele¹, E. Öjefors², K.-B. Schäd¹, E. Sönmez¹, A. Trasser¹, J. Konle³, and H. Schumacher¹

¹ Dept. of Electron Devices and Circuits, University of Ulm
Albert-Einstein-Allee 45, D-89081 Ulm, Germany

email: pabele@ebs.e-technik.uni-ulm.de

Phone: +49 731 5031593

Fax: +49 731 5026155

² Department of Materials Science, Signals and Systems, Uppsala University, Sweden

³ DaimlerChrysler Research, Wilhelm-Runge-Str. 11, D-89081 Ulm, Germany

Abstract— This paper describes the wafer level integration of a differential 24 GHz SiGe-MMIC oscillator including a buffer amplifier with a differentially driven patch antenna. The patch antenna is realized on 30 μm BCB (Benzo Cyclo Butene) used as a dielectric layer. The radiated power of the patch antenna driven by the oscillator is calculated based on measurements and the result is discussed.

I. INTRODUCTION

As the license free bands (ISM = Industrial Scientific Medical) at the lower frequency range of 2.4 GHz are getting more and more overcrowded, there is a big demand moving up in the frequency, e.g. to the ISM band at 24 GHz.

But with increasing frequency the reduction and exact control of interconnect parasitics becomes a prime concern. Due to the small wavelength there are stringent geometric tolerance requirements to avoid reflection and resonance at the interconnects [1].

On the other hand as the size of antennas shrink with increasing frequency the realization of on-chip antennas becomes feasible.

In this paper the successful integration of a 24 GHz SiGe-MMIC oscillator with a patch antenna using 30 μm BCB as a dielectric layer is demonstrated.

II. OSCILLATOR AND ANTENNA DESIGN

To realize the differential SiGe-MMIC oscillator the commercial SiGe1 process from ATMEL is used. The transistors used for this design have a selectively implanted collector resulting in an f_i and f_{max} of 50 GHz. For passive components three metalization layers are available to realize inductors, interconnects, lines, and pads. Three different resistor

layers are available for low, medium, and high ohmic resistors. One type of capacitor with a nitride as a dielectric is also available [2].

The layout of the differential oscillator with a differential cascode as buffer amplifier is shown in Fig. 1. Its topology is highly symmetric.

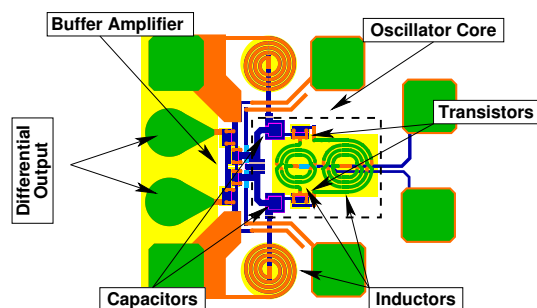


Fig. 1. Layout of the differential MMIC oscillator with integrated cascode buffer amplifier.

Two types of inductors are used, spiral inductors and center tapped (CT) inductors. While the spiral inductors are used for biasing the CT-inductors are part of the LC-tank determining in combination with the transistors and capacitors the frequency of oscillation. Due to their symmetry these inductors are compact in size and well suited for differential designs especially for feeding the biasing. The oscillator core covers an area of just $170 \times 140 \mu\text{m}^2$ while the whole MMIC has a size of $460 \times 380 \mu\text{m}^2$ including all pads for DC biasing and the differential RF output.

The output of the differential oscillator drives a differential cascode amplifier. Cascode amplifiers have a low Miller capacitance at the input and a

high backward isolation. Therefore the influence of the load to the oscillator is significantly reduced. The output of the cascode amplifier is open collector therefore the connected load must provide the biasing. This MMIC oscillator was characterized on a $50\ \Omega$ measurement system with one output port connected to a $50\ \Omega$ load resistance and the other port connected to a $50\ \Omega$ terminated spectrum analyzer. The differential oscillator has a total output power of 1 dBm and a phase noise of -104 dBc/Hz at an offset frequency of 1 MHz.

The conventional excitation of a patch antenna is either by a micro-strip line directly feeding the patch antenna or from the backside by a slot line coupling to the patch [3], [4]. The patch antenna used here is designed to be driven differentially from one side by the SiGe-MMIC oscillator. A differentially driven patch antenna connected from opposite sides is presented in [5].

As a patch antenna has normally the length of $\lambda/2$ and is open ended it has a virtual ground along its center line. Therefore it can be driven differentially by connecting feed lines symmetrically to the virtual ground, and the DC feed connection for the active device can be done along the virtual ground without a significant influence on the antenna. To verify this, simulations with HFSS and Momentum from Agilent were carried out.

An other advantage of driving the patch antenna differentially is that there is no need for connecting the ground of the chip to the ground plane of the patch antenna. This avoids parasitics caused by interconnects and simplifies the integration technology.

A photograph of the patch antenna with integrated chip and DC-pads can be seen in Fig. 3. The feed lines from the integrated chip driving differentially the patch antenna can be seen in the more detailed photograph of Fig. 4. The separation of the feeding points determines the input impedance of the antenna.

III. TECHNOLOGY

In Fig. 2 a schematic cross section of the SiGe-MMIC chip integrated with a patch antenna on $30\ \mu\text{m}$ BCB used as a dielectric layer is shown.

For the processing presented in this paper BCB serves for lots of purposes. Due to its good planarization characteristics compared to other polyimides [6] it is used for the planarization of the inserted chip to the wafer surface. The low dielectric constant ϵ_r of 2.7 and the low dielectric loss factor of $\tan(\delta)=0.0008$ [7] are important for its use as a dielectric layer of the patch antenna.

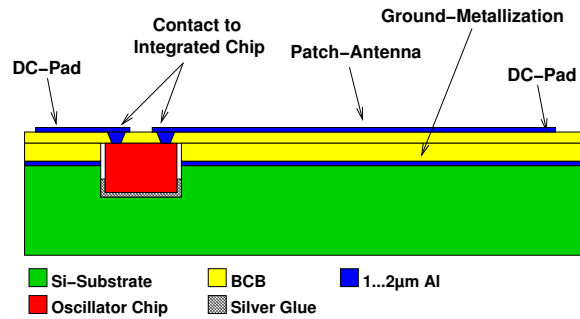


Fig. 2. Schematic cross section of the integrated oscillator chip with the patch antenna separated by a $30\ \mu\text{m}$ BCB dielectric layer from the ground metallization.

As BCB is chemically stable against phosphorous acid, H_2O_2 , and $\text{SF}_6/\text{C}_4\text{F}_8$ plasma, it is also used as a mask for etching Al, WTi, and the silicon substrate. This reduces the processing steps and the cavity is well aligned to the opening in the BCB.

For etching the windows into the silicon substrate to integrate the MMIC oscillator the time multiplexed deep etching (TMDE) technique developed by Robert Bosch GmbH [8] is used. To achieve a high aspect ratio of the side walls this etching technique switches between an SF_6 flow for etching the silicon substrate and a C_4F_8 flow for passivating the side walls.

The processing starts with sputtering 100 nm WTi and $2\ \mu\text{m}$ Al on a standard silicon substrate ($6\text{--}12\ \Omega\text{cm}$). A $22\ \mu\text{m}$ thick layer of photosensitive BCB is span onto the wafer. After exposure and developing the area where the windows for the chips to be inserted are located, the BCB is cured at 235°C for 30 min in a N_2 atmosphere. To remove residuals of BCB in the developed areas the whole wafer is etched in an O_2/SF_6 plasma. For the following processing steps BCB acts as a mask for etching both Al/TiW and the silicon substrate.

The Al is etched in phosphorous acid and the WTi is etched in H_2O_2 . Into the silicon substrate $160\ \mu\text{m}$ deep windows, for placing the MMIC chips (their height is $180\ \mu\text{m}$), are etched by the above described TMDE process. The etching rate of the process we used is $1.7\ \mu\text{m}/\text{min}$ for silicon and $21\ \text{nm}/\text{min}$ for BCB. Due to this high selectivity, BCB is well suited for masking the silicon in this process.

After etching the windows the chips are inserted and fixed using two-component silver filled epoxy. To keep the chips in place during the adhesive cure an auxiliary plate is pressed onto the wafer.

A second layer of $11\ \mu\text{m}$ BCB is spun onto the wafer. This layer of BCB planarizes between the inserted oscillator chip and the wafer surface. After exposure and developing the vias to the contact pads

of the chip and curing, residuals of BCB on the pads are removed in a O_2/SF_6 plasma. A second layer of $2\mu m$ Al is sputtered and wet chemically etched building the patch antenna and the DC connections to the inserted chip.

Fig. 3 shows a photograph of the processed patch antenna with the integrated chip and Fig. 4 a more detailed photograph to see the lines exciting the antenna and the connection of the integrated chip.

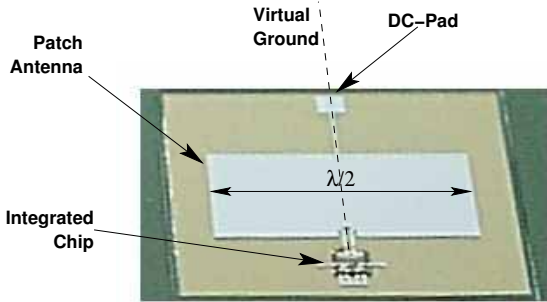


Fig. 3. Photograph of the 24 GHz patch antenna with integrated oscillator chip.

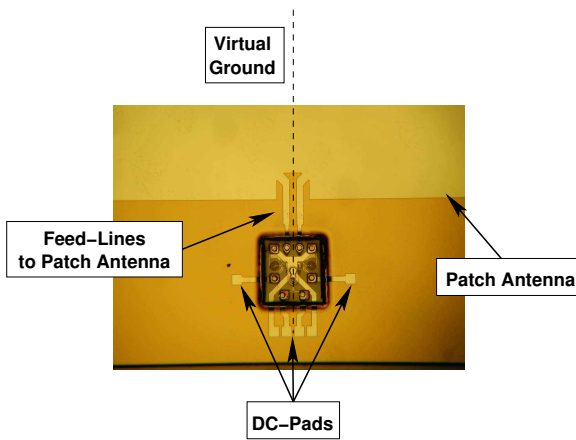


Fig. 4. Detailed photograph of the inserted oscillator chip with lines to drive the patch antenna differentially.

IV. MEASUREMENT

First the antenna without a connected oscillator chip was measured with a GS-probe. It turned out that the measured impedance of the patch antenna is much lower than the simulation results we performed with Momentum. Therefore, a simple transmission line model as shown in Fig. 5 was used.

This model consist of transmission lines terminated with end capacitances and radiation conductances. The transmission lines have the same width ($1928\mu m$) as the patch antenna and the sum of their length is the length of the patch antenna ($3848\mu m$).

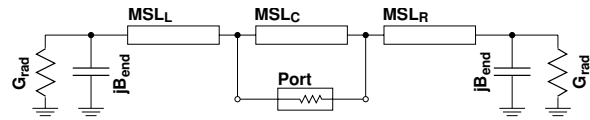


Fig. 5. Transmission line model to simulate the differential driven patch antenna.

The transmission line in the center (MSL_C) is needed to take into account that the feeding points are separated by $270\mu m$. The values for the radiation conductance and the end capacitance are calculated with following equations [9]:

$$G_{rad} = \frac{W}{120 \cdot \lambda_0} \left[1 + \frac{1}{24} (k_0 \cdot h)^2 \right], \quad (1)$$

$$B_{end} = \frac{W}{120 \cdot \lambda_0} [1 + 0.636 \cdot \ln(k_0 \cdot h)]. \quad (2)$$

To get good agreement between the simulation and the measurement two modifications were done. First the separation of the two feeding points was increased in the simulation by 20% compared to the realized structure and an additional contact resistance of two times 0.8Ω was added at the two feeding points. The simulation and measurement results are shown in Fig 6.

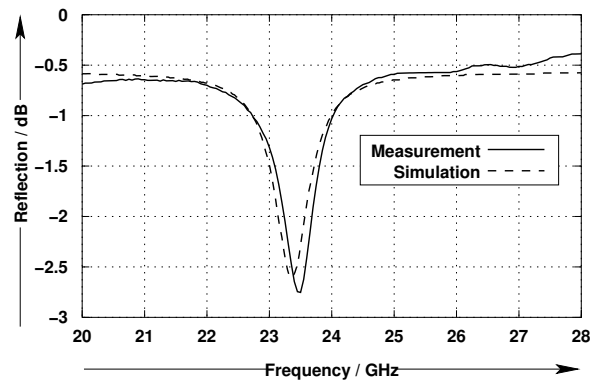


Fig. 6. Transmission line model to simulate the differential driven patch antenna.

To estimate the radiated power of the patch antenna with the integrated MMIC oscillator the radiated power was measured with a pyramidal horn antenna. The aperture of the used horn antenna is $A_p = 5 \times 6 \text{ cm}^2$ and results in a gain of 19.9 dBi, this gain was calculated according to [9]. The gain of this patch antenna was simulated with HFSS to be 7 dBi with no regards to the losses in the dielectric layer or metalization.

For calculation of the radiated power, the Friis transmission formula is used:

$$P_{rx} = \frac{P_{tx} \cdot G_{tx} \cdot G_{rx} \cdot \lambda^2}{(4 \cdot \pi \cdot R)^2}, \quad (3)$$

with P_{rx} the received power, P_{tx} the radiated power, R the distance between both antennas, and G_{tx} and G_{rx} the antenna gain of the transmitting and receiving antenna, respectively.

To be in the far field with the horn antenna the radiated power of the patch antenna was measured at a distance of 60 cm directly above the patch antenna. The measured spectrum at the horn antenna can be seen in Fig. 7 and the power is -32.7 dBm at 23.54 GHz.

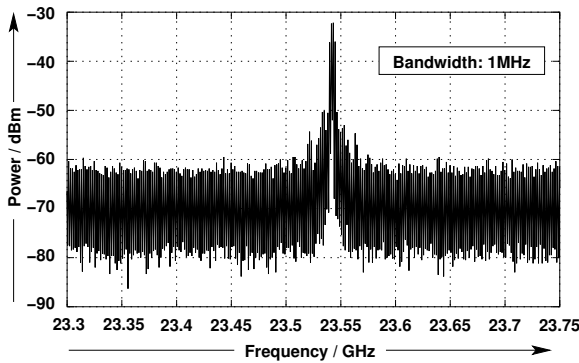


Fig. 7. Power measured with a horn antenna ($A_p = 5 \times 6 \text{ cm}^2$) at a distance of 60 cm.

With these values the total radiated power of the patch antenna is calculated with equation (3) to be -4 dBm. This is 5 dB below the output power of the MMIC oscillator measured at two times 50Ω . Reasons for this discrepancy are losses in the metalization of the patch antenna, the bad matching of the patch antenna to the output of the buffer amplifier, and the influence of the DC-needles as well as other test structures on the wafer surrounding the antenna during the measurement.

V. CONCLUSION

This paper demonstrates the successful wafer level integration of a 24 GHz SiGe-MMIC oscillator with a differentially driven patch antenna on a $30 \mu\text{m}$ thick BCB dielectric layer. As the patch antenna is driven differentially there is no need to connect the ground from the chip to the ground of the patch antenna. This simplifies the technology and avoids additional interconnect parasitics. The photosensitive BCB is also used as a mask while etching Al, WTi, and the silicon substrate successively. The radiated power of the system is calculated from measurements and the result is discussed.

VI. ACKNOWLEDGMENT

The authors are grateful to Dr. U. König from the DaimlerChrysler Research Center, Ulm and Dr. F. Bögelsack from the Department of Microwave Techniques, University of Ulm for the uncomplicated access and use of their facilities. This work was supported by the European Commission through the IST project ARTEMIS.

REFERENCES

- [1] W. Menzel, J. Kassner, and U. Goebel, "Innovative Packaging and Fabrication Concept for a 28 GHz Communication Front-End," *IEICE TRANS. ELECTRON.*, vol. E82-C, November 1999.
- [2] A. Schüppen, H. Dietrich, U. Seiler, H. von der Ropp, and U. Erben, "A SiGe RF technology for mobile communication systems," *Microwave Engineering Europe*, pp. 39-46, June 1998.
- [3] T.M. Au, K.F. Tong, K.M. Luk, and K.F. Lee, "Analyses of aperture-coupled microstrip antenna and array with an airgap," *IEE Proc. Microw. Antennas Propag.*, vol. 142, December 1995.
- [4] T. Brauner, R. Vogt, and W. Bächthold, "A Differential Active Patch Antenna Element for Array Application," *IEEE MICROWAVE AND WIRELESS COMPONENTS LETTERS*, vol. 13, APRIL 2003.
- [5] William R. Deal, Vesna Radisic, Yongxi Qian, and Tatsuo Itoh, "Integrated-Antenna Push-Pull Power Amplifier," *IEEE TRANSACTIONS ON MICROWAVE THEORY AND TECHNIQUES*, vol. 47, AUGUST 1999.
- [6] S. Bothra and M. Kellam, "Feasibility of BCB as an Inter-level Dielectric in Integrated Circuits," *Journal of Electronic Materials*, vol. 23, no. 8, 1994.
- [7] M. Mills, P. Townsend, D. Castillo, S. Martin, and A. Achen, "Benzocyclobutene (DVS-BCB) Polymer as an Interlayer Dielectric (ILD)," *Proceedings of the Symposium J on Advanced Materials for Interconnections of the 1996 E-MRS Spring Meeting Conference, Strasbourg, France, June 4-7 1996*.
- [8] F. Laermer and A. Schilp of Robert Bosch GmbH, "Methode of Anisotropically Etching Silicon." US-Patent No. 5501893.
- [9] C. A. Balanis, *Antenna Theory*. JOHN WILEY & SONS, INC., 1997.